NRC·CNRC

A computational modeling basis in support of the Canadian winter road infrastructure

NRC-OCRE-2020-TR-007

Revision 3.1
April 14, 2020

Prepared for:
Infrastructure Canada
Transport Canada
Crown-Indigenous Relations and Northern Affairs Canada

Authors:
Hossein Babaei
Paul Barrette

Ocean, Coastal, and River Engineering (OCRE) Research Centre

National Research Council Canada
Conseil national de recherches Canada

Canada

Cat. No. NR16-311/2020E-PDF
ISBN 978-0-660-34284-9

NRC.CANADA.CA

Executive Summary

In Canada, Northern communities rely on a network of winter roads – seasonal roads that only exist in the winter – for their supply of fuel, construction supplies and other bulk goods. This infrastructure is particularly vulnerable to a warming climate, especially the segments that run over frozen lakes and rivers. The safe access to floating ice covers should address three questions: How much weight is the ice able to sustain? For how much time? At what speed? Ice reinforcement has been shown in the past to be effective in making the ice cover better withstand vertical loading. The National Research Council of Canada (NRC) is currently investigating this option further by doing laboratory work aimed at improving our understanding of ice reinforcement. An ice cover, grown inside the NRC ice tank in Ottawa, has been used for the production of a series of individual ice plates resting on circular loading frames 2.5 m in diameter. Each plate is loaded vertically with an actuator while forces and displacement are recorded. In this report, we demonstrate the feasibility of computational modeling, using the structural mechanics of the COMSOL software, to simulate the mechanical response of these plates. All simulations involve scenarios with at least two planes of symmetry and are validated against the laboratory data. Both non-reinforced and reinforced ice are explored, and the boundary conditions are taken into consideration. Only the initial deflections are being investigated (within a few seconds after loading), which is dominated by the ice elastic response. The outcome of this work should guide the reader into implementing her/his own simulations, so as to generate preliminary assessments of the ice response under various reinforcement scenarios.

Table of Contents

Table of Figures

Table of tables

1. Introduction

In Canada, Northern communities rely on winter roads – seasonal roads that only exist in the winter – for their supply of fuel, construction supplies and other bulk goods. These roads relieve Northerners of isolation, and allow them to commute between communities or to access the all-weather road network in the south. There are about 10,000 km of winter roads in Canada, most of which are in Ontario, Manitoba and the Northwest Territories (NWT), and to a lesser extent in Saskatchewan and Alberta (*e.g.* Wood Buffalo Park). There are also several operations elsewhere in the country. Winter roads are typically managed by the province or the territory in which they are located, or by the local communities. The private sector (the O&G industry, pulp & paper companies, and hydro-electric companies) also builds their own roads.

Winter roads service a variety of needs:

- Goods circulation: Fuel, construction supplies, food, etc.
- Activities: Fishing, hunting, snowmobiling, etc.
- Accessing other communities for social gatherings, sporting events, etc.
- Accessing all-weather roads further south.

Winter roads are also meant to accommodate a variety of vehicle sizes, such as cars, snowmobiles, multi-axle trucks, etc. These needs and factors have to be taken into consideration in the planning, construction and maintenance of a winter road operation.

1.1. Impact of climate change

Unlike all-weather roads, which are designed and built by humans, these seasonal roads are mostly formed naturally, which is why that seasonal network is particularly vulnerable to a warming climate. This has been observed over the last number of decades, in the maximum annual ice thickness achieved during a given year, and the number of freezing-degree days (FDD)[1] available for ice growth. A large number of studies have been done on that topic (RSI, 2014, Hori et al., 2017, Hori and Gough, 2018). Figure 1 and Figure 2 provide examples of these trends. A warming climate is thought to increase the frequency and extent of warm winters. As such, it affects the safety and effectiveness of the winter road infrastructure and reduces its yearly operational lifespan. In the years during which the air temperatures are higher than normal, this has important implications, namely:

1. The road will open later, or cause mid-season closures, thereby delaying the delivery of critical supplies to northern communities.
2. Some users will expect the ice to be trafficable and may attempt to use the ice without being fully aware it is unsafe.

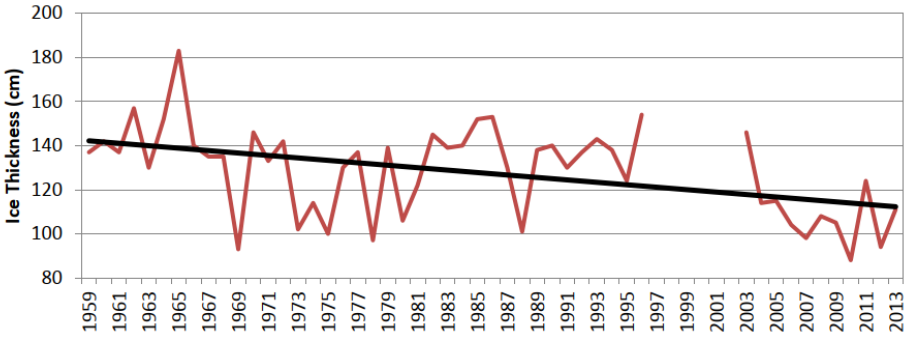

Figure 1: The variation in maximum annual ice thickness in the NWT near Yellowknife, based on data from Environment Canada, compiled by RSI (2014).

[1] FDDs is the average number of degrees below freezing point summed over the total number of days in a given time period. For instance, if the average air temperature on day 1, 2 and 3 was -5°C, -8°C and -12°C, respectively, the number of FDD for these three days is 25°C (5+8+12).

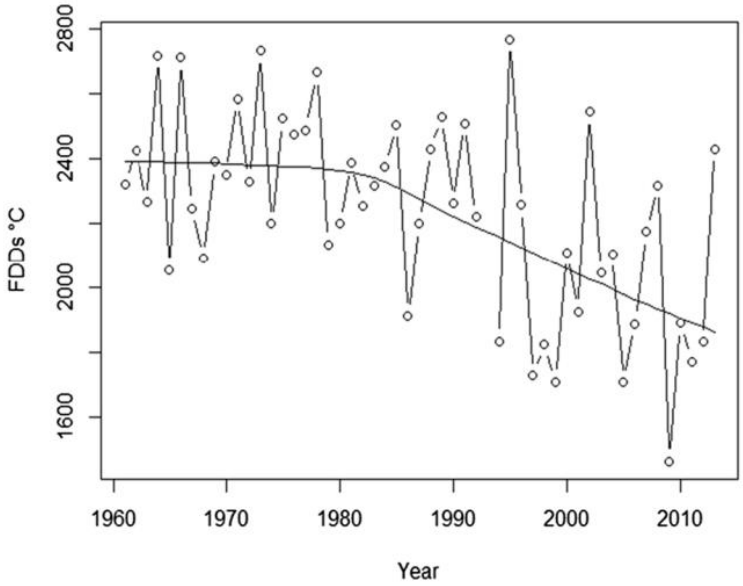

Figure 2: Reduction in the number of FDD in the James Bay region (Hori et al. , 2017).

1.2. The floating ice segments

Although winter roads run over land along most of their length, they can also comprise segments over floating ice expanses (rivers, lakes, sea) – the latter are often alluded to as ice roads, ice crossings or ice bridges. Such segments are commonly weak links in these operations because they rely on cold temperatures to achieve a thickness that is safe enough for the intended traffic. A safe ice cover is one where the buoyancy of the ice and its mechanical resistance to vertical loading provide the necessary support without failing, that is, without crack development, since these can lead to a breakthrough. Breakthroughs occur every year – in a number of cases, they have led to fatalities.

1.3. Objective of this report

The main objective of this report is to introduce the reader to the capability of computational modeling, validated against laboratory tests, for predicting the response of an ice cover, with or without reinforcement, submitted to vertical loading. This will be addressed in Sections 4 and 5. In order to achieve this objective, the reader will be provided (Section 2) with a basic understanding of what needs to be considered in assessing what a safe ice thickness should be for the floating ice segments. Afterward, the concept of ice reinforcement will be introduced, and its potential to mitigate risks of breakthroughs will be discussed (Section 3).

1.4. Target readership

The target readership for this report are students and researchers that are not familiar with the winter road infrastructure, particularly the segments that run over floating ice. The report is aimed at providing sufficient information on these structures so as to encourage others to further develop the computational capability of the tools described herein, explore the potential of these tools and conduct further analyses.

2. Assessing the safety of floating ice covers

This section offers a brief summary on the nature of the forces exerted on a floating ice cover that is used for surface transportation. Three characteristics of ice that set this material apart from others known to the structural engineering world:

1. Ice creeps with time. For instance, if a vehicle is parked onto an ice cover (i.e. ‘static loading’), it will slowly deflect downward with time.

2. Ice is also known to be brittle. Using the above example, at some point, the parked vehicle can break through the ice cover, due to the propagation of crack networks.
3. Ice is less dense than its liquid phase, and hence floats on the water below it. A vehicle traveling on floating ice can induce a loading regime ('dynamic loading') that is quite unlike that existing in an asphalt or concrete road and associated grade and sub-grade.

More information on the above is provided elsewhere (Barrette, 2015). We will now look at what these few considerations imply from an operational perspective.

2.1. Understanding the loading regimes

The safe access to floating ice covers should therefore address three questions:

1. How much weight is the ice able to sustain?
2. For how much time?
3. At what speed?

2.1.1. How much weight is the ice able to sustain?

When an ice cover is pushed downward as is the case when it supports a load – *e.g.* a vehicle - it sinks under the load (Figure 3). As it does so, and assuming it is freely floating, it displaces a volume of water whose weight is equivalent to that of the vehicle. This is known as Archimedes' principle.

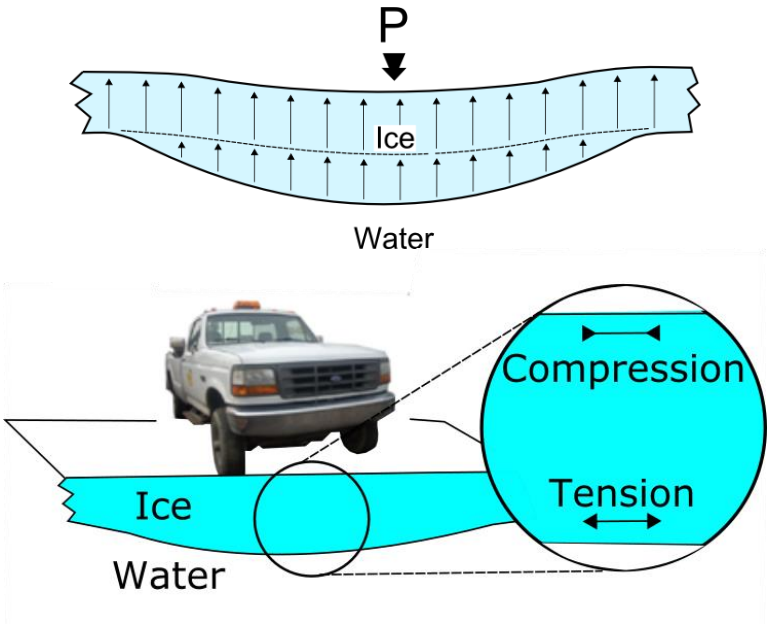

Figure 3: Top) Resistance to sinking of a floating ice cover under load, P, from the ice buoyancy, is increased by the resistance to flexure (after CRREL, 2006). Bottom) This establishes a complex regime of stresses inside the ice cover.

In the 1950s, Lorne Gold, a scientist with the National Research Council in Ottawa, was looking for a way to help winter road users determine how much weight an ice cover of a given thickness could safely sustain. Analytical methods already existed at the time (and are still being used by engineers and scientists). However, they were relatively complex and thus not practical for stakeholders who did not have a sufficient technical background. These methods also made assumptions (*e.g*. uniform ice, no cracking) that were not representative of real ice.

Gold collected information from the pulp and paper industry on breakthroughs that had occurred, including data on ice thickness and weight, of the loads that caused the ice to fail (Gold, 1960, 1971). From this information, he used a formula in conjunction with the breakthrough data to come up with a method that, to

this day, is used as a guideline for floating ice, including ice platforms and landing strips. This formula has the following form:

$$P = Ah^2$$

Where

P: Design load
A: Empirical parameter with pressure units
h: Ice thickness

The parameter *A* is related with the ice flexural stress. The value assigned to it varies widely. The thickness *h* is assumed to be representative of the ice (road) as a whole (or a section thereof) with due consideration to prospective variations.

With this formula, a plot can be produced, as shown in Figure 4, that can be used as guidance to determining what a safe load could be for a given ice thickness. The 'A' values used by Gold in this plot are 3.5, 18 and 70 kg/cm^2, retained for the following reasons:

- The first value was the lower bound value for reported breakthroughs, *i.e.* none (or few) occurred below this line.
- The second value is the upper bound value for successful use of ice covers, *i.e.* these cases all plot below that line.
- The third value is a line acting as an envelope for his observations, i.e. failures were observed for conditions up to this line.

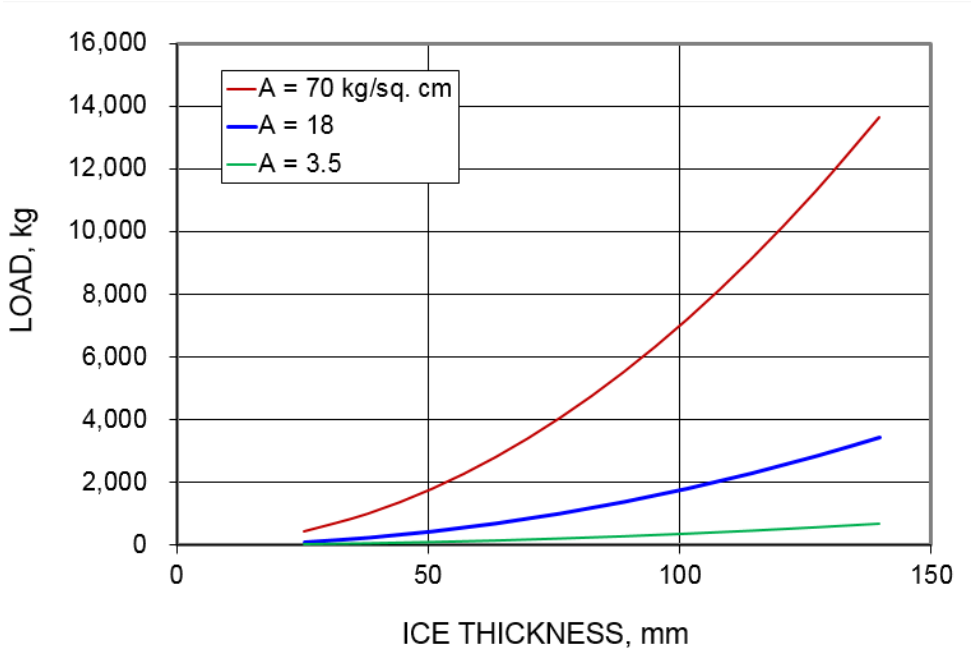

Figure 4: Load as a function of ice thickness for the three different A values used by Gold (1971).

Although simplified, these considerations capture some of the fundamentals of ice road design. Referring back to Figure 3, this means the required ice thickness below the pick-up truck (assuming a weight of 2000 kg) would be about 110 mm if we accept A as 18 kg/cm^2.

It should be borne in mind that Gold's formulation is based on empirical evidence, *i.e.* observations of real events, not solely on theoretical concepts. It is a curve-fitting exercise – a best-fit line describes the relationship between two parameters, namely ice thickness and loads. This line may be seen as an 'envelope'. Above it, the probability of a breakthrough caused by a number of factors (localized thin ice,

presence of a crack, high vehicle speed, etc.) is deemed unacceptable by the guideline. Figure 5 is an example of a breakthrough for which the ice thickness was, theoretically, reportedly thick enough to withstand the load of the vehicle (the vehicle would not have been allowed on the road otherwise). Figure 6 shows an example of cracks in a natural ice cover – it has not yet been shown to what extent these could contribute to weakening the ice.

Figure 5: An incident in March 2016 on an ice crossing near Deline, NWT. The circumstances that led to this incident are unknown to the authors. The fracture pattern suggests that pre-existing cracks may have played a role (photo courtesy of NWT Environment and Natural Resources.

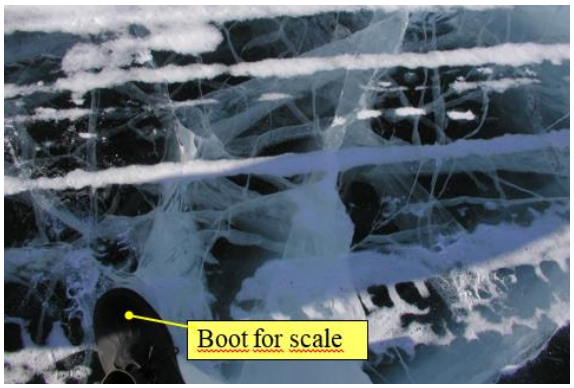

Figure 6: Cracks are usually present in ice covers (photo taken by one author on Gordon Lake, in the NWT).

2.1.2. How much time should a vehicle remain on the ice?

Gold's formula is not meant to be used for loads that remain at one location for a certain time period. The reason is that, after a certain amount of time, failure of an ice cover could occur. That is because, with time, stresses induce non-elastic deformation in the form of micro-cracks (e.g Sinha, 1989b), which develop into large cracks and, ultimately, breakthrough.

In general, the heavier the load, the less time it should be allowed to remain on the ice. As to what the length of that time period is, different guidelines have different recommendations. Some, for instance, specify that Gold's formula should only be used for moving loads (CSAO, 2009, Government of Manitoba, 2014). Others specify a two hour limit (CSST, 1996, IHSA, 2014), which is also what Gold (1971, p. 179) prescribed.

If a load has to remain on the ice, some guidelines advise to monitor the freeboard (Frederking and Gold, 1976, Sinha and Cai, 1996) by drilling a hole through the ice. When the water level reaches the ice surface (*i.e.* the freeboard reduces to zero), the load has to be removed. This practice is supported by the analyses of Frederking and Gold (1976) and has been validated by many sources (*e.g.* CSST, 1996, Masterson, 2009, IHSA, 2014). BMT Fleet Technology (2011) recommends to use a time-dependent reduction factor if the load duration is to exceed 15 minutes – the longer the duration, the lower the allowable load. Figure 7 is a recent example (January 2020, near Vladivostok in Russia) of what was likely a case of time-dependent ice failure. At least 20 vehicles that had 'safely' parked on the ice during an ice fishing event eventually went through it[2]. Fortunately, this occurred next to the shoreline, where the water was shallow.

[2] https://www.lapresse.ca/actualites/insolite/202001/06/01-5255846-peche-surprise.php

Figure 7: Two of the 20+ vehicles that had been parked on the ice surface before breaking through it. This can be attributed to the time-dependent reaction of the ice cover.

2.1.3. What is the maximum speed?

The pattern of the ice deflection due to the motion of a vehicle depends on the vehicle speed. At low speed, there are 'deflection bowls' in the close vicinity of the vehicle (Figure 8). As the vehicle speed is increased up to 'critical speed', flexural-gravity waves appear in the ice extending hundreds of meters away from the vehicle. At constant velocities with speeds higher than the critical speed, these waves appear standing to the driver of the vehicle over a lake of uniform depth and ice of constant thickness.

The critical speed u_c depends on water depth (W), ice thickness (h) and ice stiffness (elastic moduli). The latter two parameters contribute to a parameter called the characteristic length, L:

$$L = \frac{{Eh^3}/{[12(1-\nu^2)]}}{\gamma_w}$$

In this equation, *E* is the effective[3] elastic modulus, *h* is the ice thickness, ν is Poisson's ratio for ice and γ_w is the specific weight of water.

For $W > L$, then $u_c = 1.25(gL)^{0.5}$
For $W < L$, then $u_c = (gW)^{0.5}$
where *g* is the gravitational acceleration (CRREL, 2006). This means that in shallow waters, the critical speed is independent of ice thickness and stiffness.

The presence of such waves has been documented by van der Sanden and Short (2016) and shown to agree with theory (Babaei et al., 2016)(Figure 9).

There is a large amount of research done on moving loads over floating ice covers (*e.g.* Squire et al., 1996, Van Der Vinne et al., 2017, Dinvay et al., 2019), however it is relatively complex and still poorly understood. At this time, the guidelines provided by the Government of the Northwest Territories (Government of the NWT, 2015) provide good guidance in terms of vehicle speed and spacing between vehicles.

[3] An 'effective' modulus is typically lower than the Young's modulus, because the deformation is not strictly of an elastic nature (see later for additional comments).

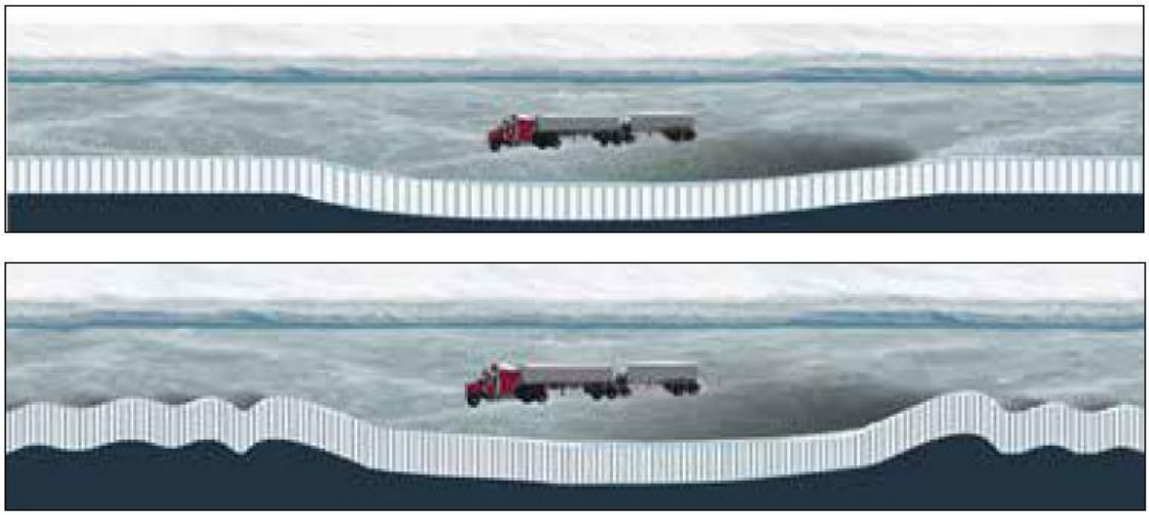

Figure 8: Top) At relatively slow speed, the bowl below the vehicle moves with it. Bottom) At critical speed, a steady wave is establish ahead of the vehicle (i.e. it moves at the same speed as the vehicle), which amplifies the deflection (from Government of the NWT, 2015, Figs. 3.3 and 3.4).

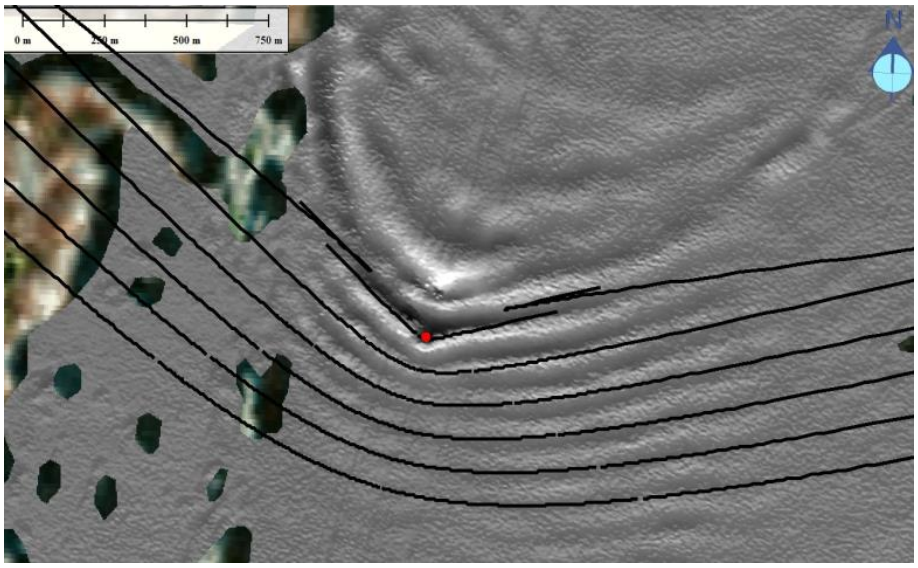

Figure 9: Wave patterns viewed from above (satellite imagery) on a lake in the NWT. The red dot is the travelling vehicle, and the black lines are the theoretical wave patterns (Babaei et al. , 2016).

3. Toward an engineering solution

Contractors and engineering consultants have a wealth of knowledge and experience, and take various corrective measures to make optimum use of the winter season and address the issues causing road closures. Ice growth via artificial flooding and/or spray icing are common techniques, but these are becoming insufficient in the face of climate change. A means of mitigating the effects of climate change on static or dynamic loading should be sought.

One promising solution to this challenge is to incorporate an engineered material into the ice cover (Figure 10) – this is discussed further elsewhere (Barrette et al., 2019, Charlebois and Barrette, 2019). Such a solution could achieve a number of goals:

- It would increase the bearing capacity of the ice.
- It would do so in a predictable fashion.
- Even if the ice does fail, the reinforcement material inside the ice would support the load, thereby preventing breakthrough.

This solution would become a tool available to operators to strengthen known weak links and prevent these locations from shortening the road's yearly operational lifespan.

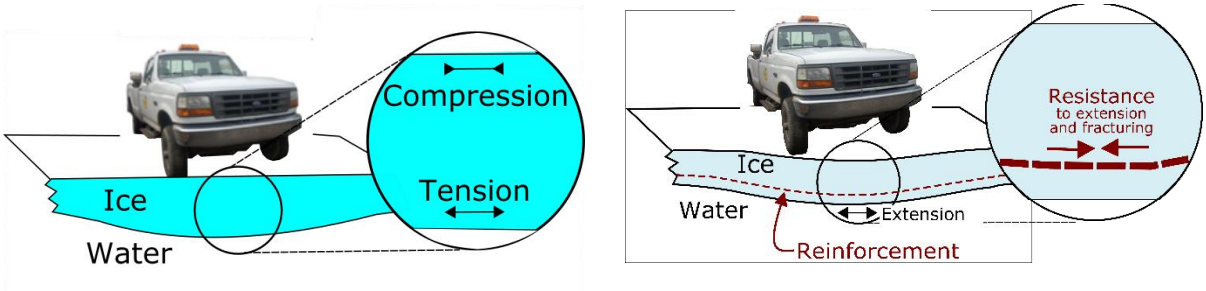

Figure 10: Left) Stress regime inside an ice cover loaded vertically. Right) Incorporation of a reinforcement inside an ice cover, to increase its resistance to the extensional component.

Ice reinforcement has been used in the past in winter road operations (*e.g.* Gold, 1971, Michel et al., 1974). It has also been tested in the field and in the laboratory. Cederwall (1981), using steel bars, and Haynes et al. (1992), with a polymeric mesh, are examples of macro-reinforcement. Kuehn and Nixon (1988), with sawdust, Nixon and Weber (1991), with alluvium, and Gold (1993), with wood pulp, offer examples of micro-reinforcement. However, these techniques (micro- or macro-reinforcement) have never been made formally available to winter road operators, partly because they require further investigation.

3.1. How does reinforced ice work?

Provided the reinforcing material adheres well to the surrounding ice and has an elastic modulus higher than that of ice, it can improve the resistance to ice failure (*i.e.* resistance to first crack). If, as expected from most reinforcing material, it does not itself yield, then it will improve resistance to ice breakthrough, and should also prevent it. What this means is that, even after sustaining extensive cracking, a reinforced ice cover can still play a critical role (by preventing a vehicle from going through the ice).

It is therefore important to distinguish two terms – *ice failure* and *ice breakthrough* – because they have different consequences from an operational standpoint (for additional information about all operational aspects, the reader is referred to Government of the NWT, 2015). The following is a description of what these terms mean.

3.1.1. Ice failure and 'first crack'

The term *ice failure* assumes a perfect elastic response and implies the formation of a 'first crack', *i.e.* the initial cracking activity in the ice. That notion is a simplification of reality, but it is helpful in understanding the ice response to vertical loading. Not permitting a first crack is also an industry standard (e.g. Masterson, 2009). For application to a real ice operation, this first crack may allow the water to seep its way upward through the ice cover, causing local flooding on the ice surface, which causes additional loading. At that point, the ice cover is deemed unsafe. It is closed to traffic and may be artificially flooded further, until the ice freezes again. In the meantime, if there is enough room, an alternative routing is built around that zone. The guidelines for the determination of a safe ice cover thickness are based on first crack.

As will be seen later, with or without reinforcement, failure occurs immediately after a peak load in a plate test, which is also the maximum load the plate will see. The stiffer the reinforcing material, the higher the load required for first crack. A higher volume ratio of that material will also increase resistance to first crack.

3.1.2. Ice breakthrough, work and resilience

In a real scenario, *ice breakthrough* is beyond failure, and basically refers to the collapse of the ice cover at the point of load application. For a breakthrough to occur, the vertical weight exerted on it is sufficient

not only to achieve first crack, but also to cause the vehicle (or person, or object, etc.) to go through the ice, either partially (*e.g.* one vehicle axle) or fully. It is the ultimate and unfortunate outcome of an ice cover that is unable to support the load, and may lead to equipment loss, injury or death. This breakthrough is expected to occur after a network of cracks has developed in the ice, namely radial and circumferential. The energy expended in generating this crack network is referred to as *work*, and the resistance to breakthrough is referred to as *resilience* (*i.e.* the amount of work the ice can absorb before breakthrough).

3.2. The role of laboratory testing

The laboratory test program was meant to simulate as closely as possible real scenarios inside an environmental chamber, so as to have full control of the temperature regime. This was required for the production of the ice as well as for the actual mechanical testing. Using adequate instrumentation, as described later, the data produced can be used to validate the computational modeling.

3.3. The role of computational modeling

The computational studies that have been conducted to date (Lau, 2017) on ice reinforcement were done on a trial-and-error basis, in the days where computational means were not as powerful, versatile and available as they are today. Since then, advances in computational modeling have been made, and this tool is now used routinely to guide structural designs in a large number of engineering fields. In ice engineering, it has not yet achieved the same level of application (Bergan et al., 2010) – however, investigations have been done in that regards, some directly relevant to floating ice covers (Lau, 2017).

In this report, we will describe a methodology for computational modeling that is capable of reproducing the actual ice behavior, both without and with reinforcement. This methodology only addresses the resistance to ice failure, not the resilience to breakthrough, *i.e.* it will *only* explore the initial (elastic) response of the ice, *before* cracking activity begins. Optimizing the ice cover resistance to first crack is seen as an important first step – it is also the simplest to model, since it only factors in the time-independent response of the ice, *i.e.* within the elastic domain. Although the outcome of this work is preliminary, it points to a tool that shows promise in terms of being able to explore reinforcement options.

4. Laboratory testing

The purpose of this section is to provide the reader with information about laboratory testing of reinforcement of ice covers at NRC. This test series serve as the basis for validation of the computational model, the third objective of this report. The testing done so far is preliminary – additional testing will be conducted in the near future, using the same methodology.

4.1. The reinforcement materials

The choice of materials used for reinforcement was based on the outcome of an earlier inquiry (Charlebois and Barrette, 2019) (Figure 11):

- Triaxial TX7 geogrid, by Tensar International
- Several parallel strands of steel cables 3.2 mm and 6.4 mm in diameter

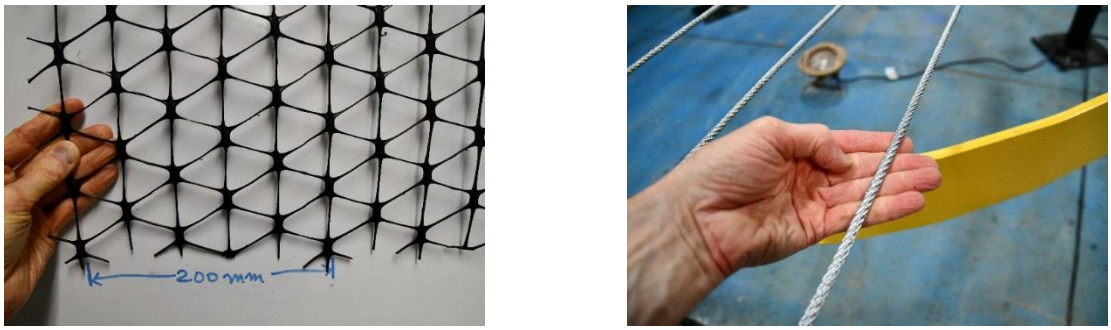

Figure 11: The two reinforcement materials used for plate testing: Left) Geogrid. Right) Steel cables.

4.2. Procedures

All test were done in NRC's ice tank in Ottawa, a concrete basin 21 m in length, 7 m in width and 1.1 m in depth. It is equipped with a carriage, which is a structure spanning the full width of the tank, traveling on rails, and used for towing or for carrying instrumentation and actuators. The ice tank is enclosed in a chamber in which the temperature can be reduced to -20°C. A four-step procedure was adopted to conduct these tests (Figure 12).
:

1. Installation of eight 2.5 m diameter load frames, and of the reinforcement above them (Figure 13).
2. Water in tank cooled down and seeded ice (columnar-grained S2) was allowed to grow downward to enclose the reinforcement (Figure 14).
3. Cutting individual ice plates from the ice sheet above each frame, and lowering the water level to allow the plate to rest on them (Figure 15, Figure 16).
4. Removal of the remaining water and applying a vertical load to the center of the plate.

The aim was to have the ice plate resting freely on the frame below it before testing, *i.e.* without being bonded (ad-frozen to it) or otherwise restricted along the frame's circumference. Available evidence shows that this was mostly achieved only for some tests; for others, as will be discussed later, the ice plate was frozen onto the frame.

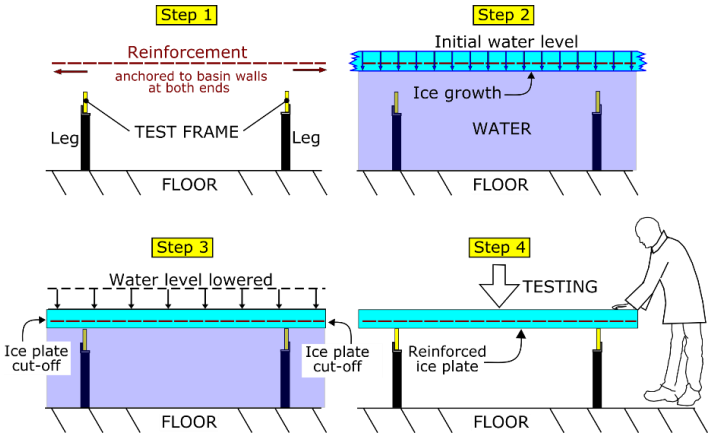

Figure 12: Four-step procedures designed and implemented for plate testing of reinforced ice. For Step 4, an actuator has been used to deliver the vertical force.

4.3. Instrumentation

The instrumentation included:

- An actuator, consisting of a 95 kN capacity hydraulic piston and a 45 kN capacity load cell. The actuator, which also incorporated a transducer to monitor displacement, was used to apply the load onto the ice at a desired displacement rate (1.4 mm per second), via a circular platen 100 mm in diameter that was connected to the load cell (Figure 17).
- Six spring-loaded linear variable inductance transducers (LVIT), with a 0-50 mm range and a 0-10 volts DC output, and an accuracy of 0.01 mm. These were used to monitor ice deflection (Figure 17).
- An acoustic emission system, consisting of a two-channel system and one sensor. It was a wideband frequency sensor, with an operating frequency range of 200-850 kHz. This system was used to monitor cracking activity (Figure 17, Figure 18).
- Data acquisition for load and displacement sensors was done at a rate of 500 Hz (*i.e.* 500 readings per seconds).
- A temperature profiler to monitor the temperature of the water, the ice and air, at a given location in the ice tank. That location was away from all tests. The target ice temperatures was -5°C.

Figure 19 is a simplified depiction of the test set-up.

Figure 13: Lay-out of circular frames in the OCRE ice tank, and of the reinforcement above them (person for scale at far end).

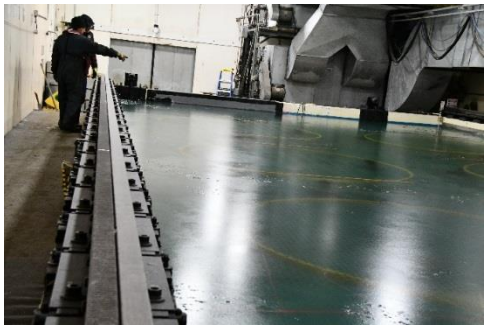

Figure 14: Tap water brought into the tank was cooled down and seeded. The yellow frames can be seen through the ice.

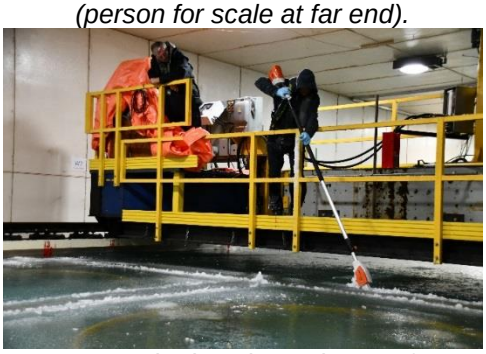

Figure 15: Once the ice above the test frames had achieved target thickness (thereby incorporating the reinforcement), it was cut around each test frame. This was done from the ice tank carriage straddling the ice tank.

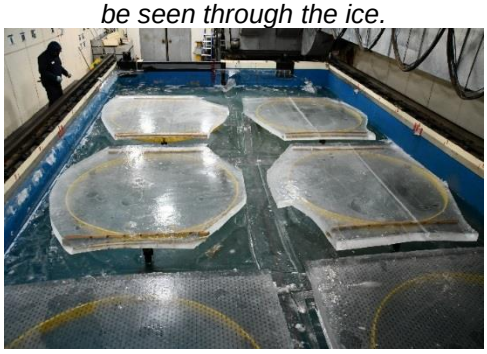

Figure 16: View of ice plates resting on the yellow frames, ready for testing (person at upper left for scale).

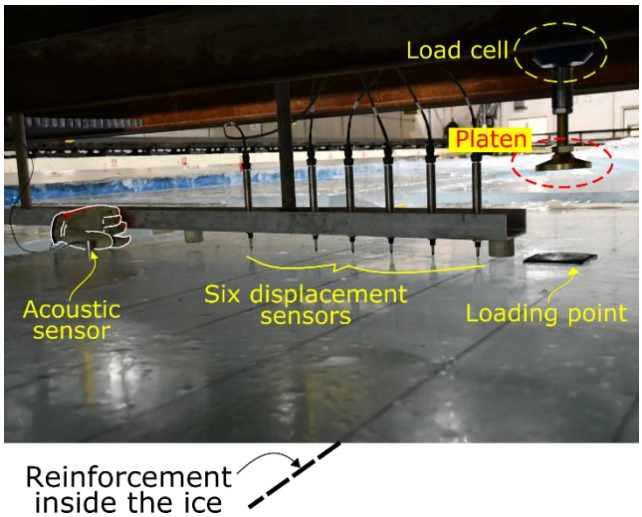

Figure 17: Instrumentation set-up below the carriage, here for a test done on ice reinforced with steel cables.

Figure 18: Close-up view of the acoustic sensor, here on ice reinforced with the geogrid.

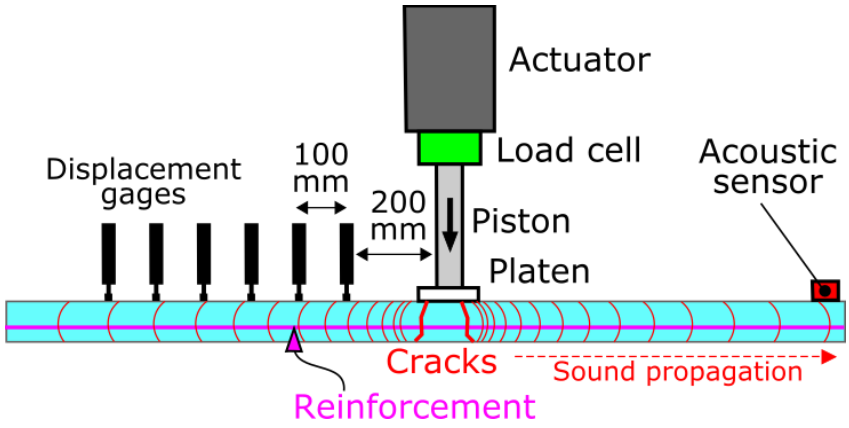

Figure 19: Schematics of instrumentation set-up (not to scale). Each crack generates a sound wave inside the ice, which is recorded by the acoustic sensor.

4.4. Preliminary testing

A total of eight preliminary tests were conducted, one on each ice plate and labelled W1 to W4 and E1 to E4 (Table 1). Two types of boundary conditions were defined for the tests (Figure 20):

- Simple support, no vertical deflection of the ice plate at the circular frames.
- Rotation and all displacements fixed over the penetration depth B of the circular frame into the ice plate (see Figure 20).

The tests where both motions were allowed are considered simply supported. They contrast with the tests where these motions were not allowed (N)(Figure 20).

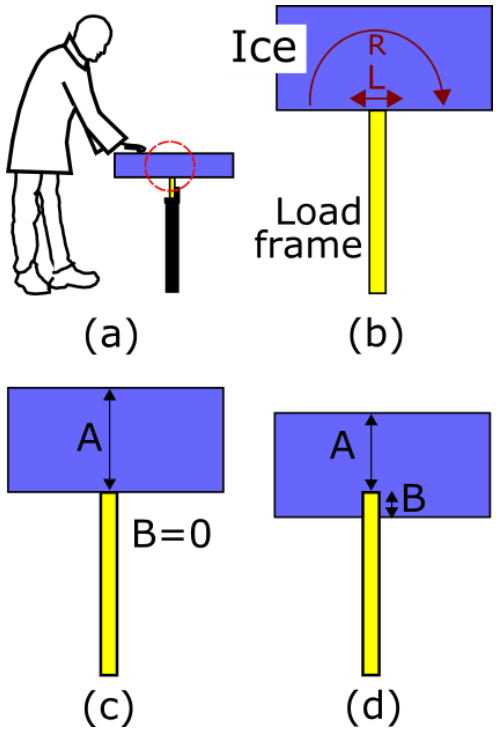

Figure 20: In this experimental work, the nature of the interaction between the ice plate and the load frame (a) led to different levels of restriction along that interface. As shown in (b), these are divided into: rotational (R) and lateral (L). In (c), the ice lies on top of the frame. In (d), the frame penetrates into the ice – A is the thickness of the ice above the frame, and B is the penetration depth. These parameters were used as inputs for computational modeling.

Table 1: Information on tests. Boundary conditions are shown in the third column (N: no rotation allowed, R: rotation allowed, L: Lateral motion allowed).

Test	Reinforcement	Boundary conditions	Remarks
W1	None	R,L	No data acquired due procedural error
W2	Geogrid	R,L	
W3	Steel cables	R,L	7 strands, 3.2 mm diameter
W4	Steel cables	R,L	10 strands, 6.4 mm diameter
E1	None	N	
E2	Geogrid	N	
E3	Steel cables	N	7 strands, 3.2 mm diameter
E4	Steel cables	N	4 strands, 3.2 mm diameter

There was a substantial difference between un-reinforced and reinforced ice. The former underwent an instantaneous breakthrough (within one second of load applications), via a set of radial cracks (Figure 21). The reinforced ice showed considerable resilience to collapse. For a test done on the geogrid-reinforced ice (Figure 22) a set of radial cracks developed within 2-3 seconds of load application, which was followed by additional radial cracking. Limited circumferential cracking then occurred within 400 mm of the load application point, alongside progressive shearing along existing cracks. Near the end of the loading event, cracking was concentrated around the platen, to a point where it was driven through the ice surface (see Figure 22 at the very center of the ice plate). A similar scenario was observed with the cable-reinforced plates, with the difference that, as the loading event unfolded, shearing along the cables became a significant load-accommodating factor. Some of that shearing occurred preferentially at the intersection of a cable and a crack surface (Figure 23).

The instrument response for one test is shown in Figure 24 as an example. A relatively good correlation between load and cracking activity can be observed, with the largest load drops often generating the most acoustic emission (AE) counts – each count was assumed to represent a cracking event. Figure 25 shows the ice surface deflections recorded by the LVITs, at three time intervals very early in the loading event. The general downward deflection trends are seen, but it is uncertain as to why these trends are not smooth, as one might expect. A closer inspection of the load and AE responses (Figure 26) shows that no cracking activity occurred before the very first peak load, which occurred in this case about 4 seconds after load application.

4.1. Data used for validation of the computational model

The short-term response (such as shown in Figure 26) is the most relevant for the computational modeling exercise in this report. The rationale behind this is that it is dominated by linear, time-independent deformation processes, *i.e.* those of elastic nature. They are much simpler to model and yet can offer very helpful insights in the understanding of plate response. This is seen as a first step in that modeling exercise.

4.2. Cracking activity

Cracking activity, monitored by the acoustic system, provides information on non-elastic deformation. It helps to verify that cracking is minimal and does not contribute substantially to the short-term response. As can be seen in Figure 26, very little evidence of cracking activity is recorded by the acoustic sensor before the first peak in the load trace. The full data set (on the entire ice response) will be instrumental in later analysis of the ice longer-term response, and will provide insights on plate resilience to breakthrough.

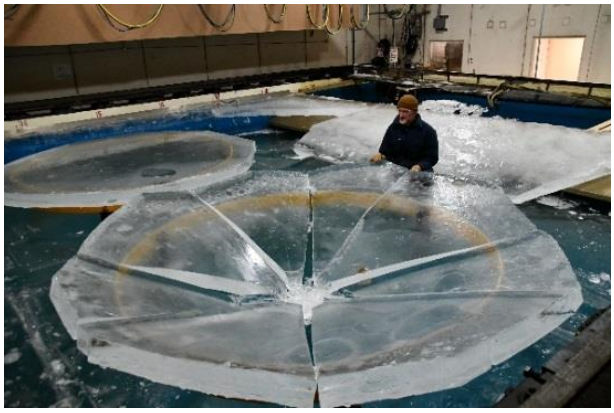

Figure 21: Outcome of a test done with non-reinforced ice. Person for scale.

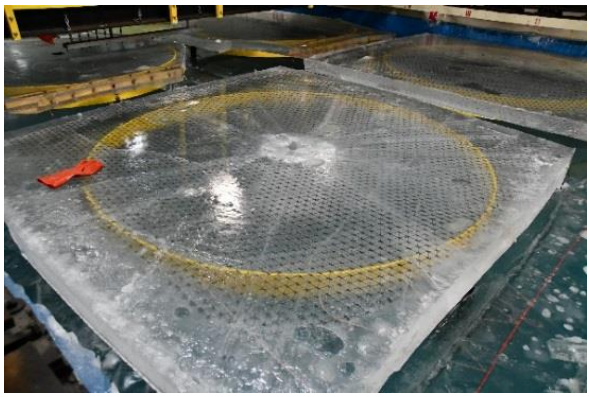

Figure 22: Outcome of a test done on an ice plate reinforced with the geogrid.

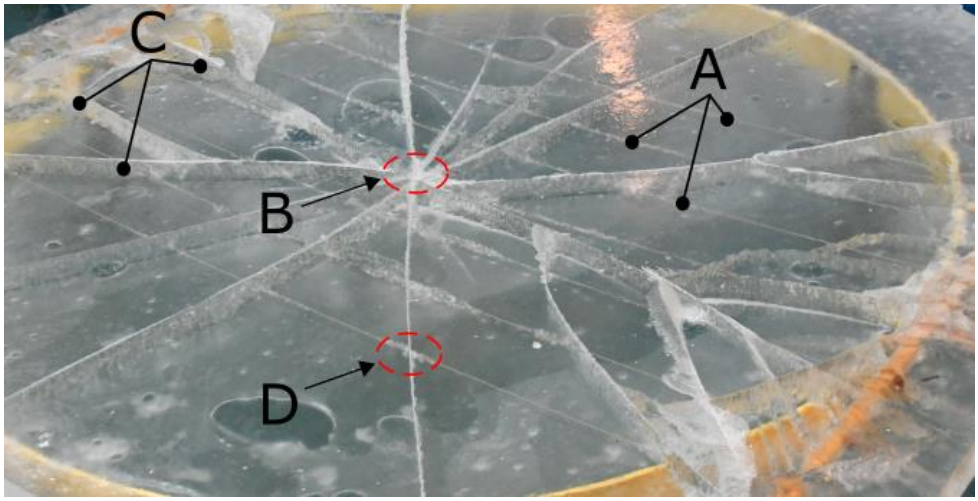

Figure 23: Outcome of a test done on an ice plate reinforced with the steel cables. A: Three cables (out of seven for this test), B: point of load application, C: examples of radial cracks, D: example of shearing along the cables, here initiating at the intersection with a cable.

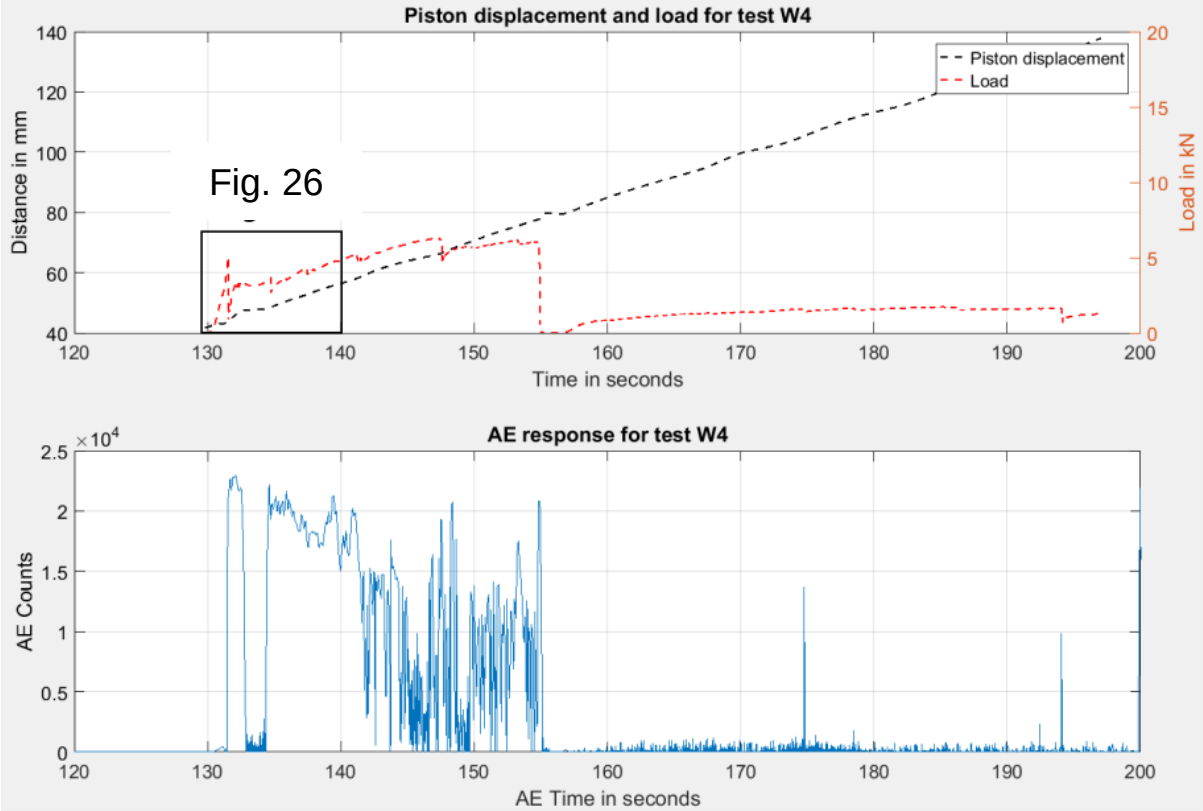

Figure 24: Example of instrument response: Top) Piston displacement, load response and deflection vs time - the rectangular inset lower left corresponds to Figure 26; Bottom) Synchronized AE emission.

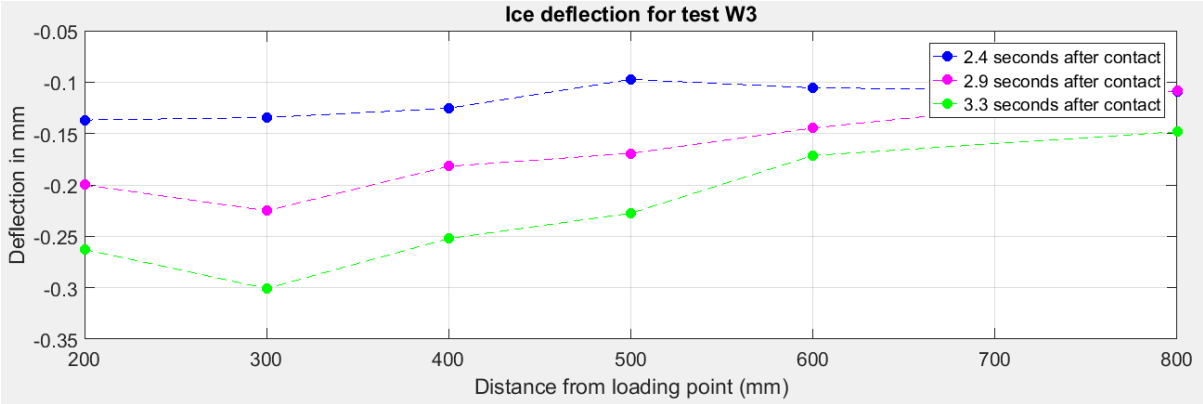

Figure 25: Ice deflection vs distance from the loading point at three different time intervals for the same test.

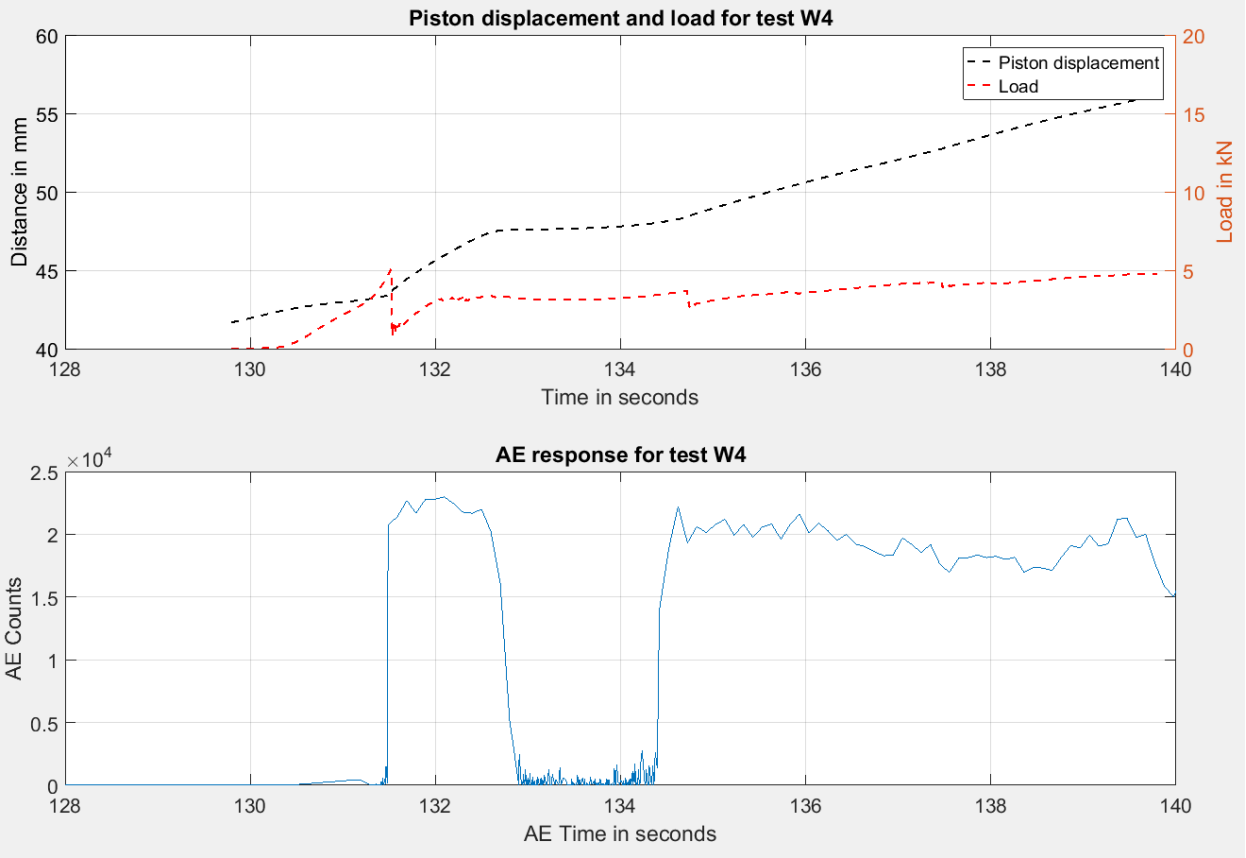

Figure 26: Same as in Figure 24, but very early in the loading event (see inset in that figure).

5. A computational modeling tool

The structural mechanics module of COMSOL Multiphysics© (COMSOL AB, 2014) simulation software was used for the present computational study. COMSOL is a general purpose finite-element modeling toolbox with the capability to simulate scenarios involving coupled physics with modules such as Fluid Flow, Heat Transfer, and Acoustics. The reason for the selection of this commercial toolbox was its capability and availability.

5.1. Procedures

The geometry of all computational simulations in this report is a horizontal circular plate with a diameter of approximately 2.5 m and, unless mentioned otherwise, a thickness of 0.12 m. The ice plate is loaded vertically on the top, over a central circular surface area 0.1 m in diameter. Because of the symmetry of material distribution, geometry, loading, and boundary conditions, all simulated cases are also symmetric problems with at least two perpendicular planes of symmetry. In virtue of this symmetry, we only simulate a quarter of the circular geometry to reduce computational time. Unless mentioned otherwise, the lower circular edge of the plate is free to move in the horizontal plane but fixed in the vertical direction. This boundary condition is known as ‘simply supported’. Geometric and material nonlinearities of the ice and reinforcement entities have been neglected in all present simulations and, as mentioned earlier, only the linear elastic response of the system is solved for. Additionally, the problem is treated as three-dimensional. Figure 28 shows the geometry, boundary conditions and loading condition for a non-reinforced, simply supported case.

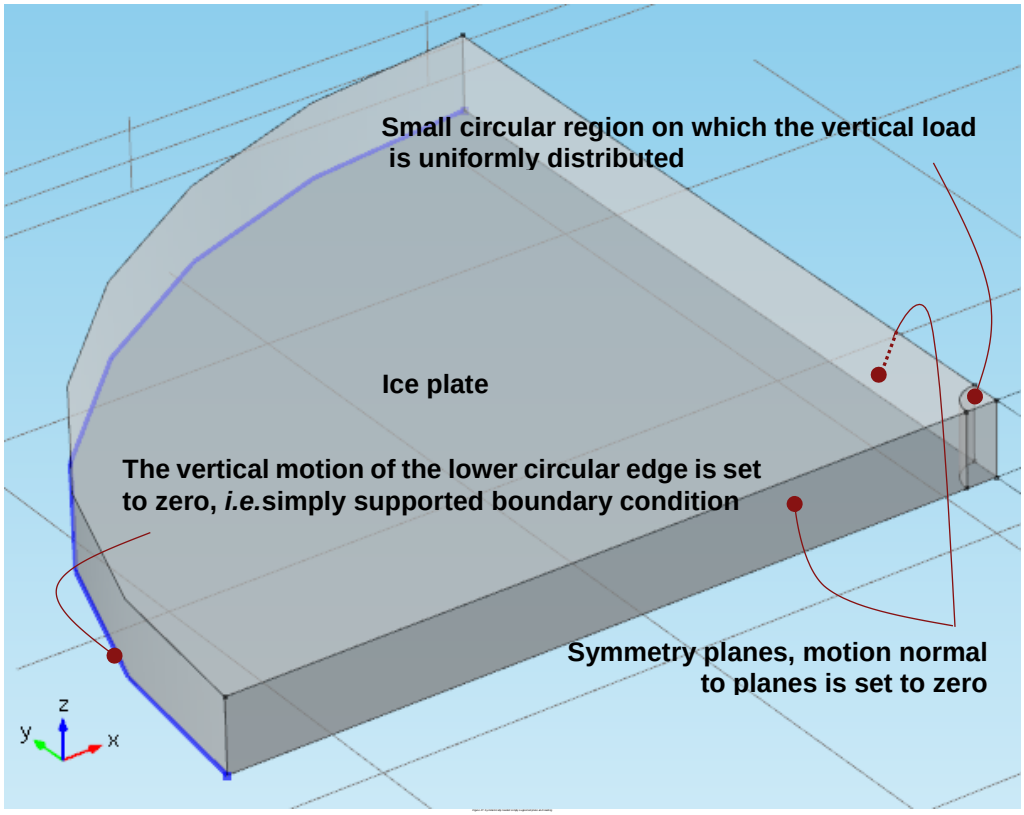

Figure 28. All simulations involve scenarios with at least two perpendicular vertical planes of symmetry. The plate is loaded vertically over a small horizontal central circular region. Unless mentioned otherwise in this report, the lower circular edge of the plate is only free to move horizontally. Note the xyz axes at the bottom left.

We proceed with the verification of the boundary conditions and the present computational finite-element tool. The exact vertical deflection of an isotropic and homogenous elastic thin circular plate (Timoshenko and Woinowsky-Krieger, 1959) loaded uniformly centrally over a small circular region, simply supported on the outer edge, is provided in Young and Budynas (2002):

$$w = -\frac{P}{16\pi D}\left[\frac{3+\nu}{1+\nu}(a^2 - r^2) - 2r^2 ln\left(\frac{a}{r}\right)\right] \qquad \text{for } r > r_o$$

$$w_{max} = -\frac{Pa^2}{16\pi D}\frac{3+\nu}{1+\nu} \qquad \text{for } r = 0$$

in which $w, a,$ and r denote vertical deflection, radius of the plate, and the radial coordinate, ln represents the natural logarithm function, P is the vertical load, distributed uniformly over a small circle of radius r_o, and the flexural rigidity *D* of the plate being equal to $Eh^3/\left(12(1-\nu^2)\right)$ with h, E, and ν being the thickness, Young's modulus and the Poisson's ratio of the ice plate. Poisson's ratio in all simulations was 0.33.

We simulated the non-reinforced ice plate loading shown in Figure 28 and compared the vertical deflection with the calculated deflection given in the above equations. From a computational perspective, this represents an 'exact' solution (as opposed to 'approximate')(e.g. Aandahl et al., 2014). The load (P) and Young's modulus are, respectively 3000 N and 3 GPa. The latter value (for the modulus) will be justified later.

Figure 30 shows the comparison of the exact and simulated deflections for different finite-element mesh resolutions. 'Fine', 'finer', and 'extra fine' meshes in the present verification case are associated with

approximately 220k, 688k, and 2748k elements, respectively. Regardless of whether the finite-element mesh is ‘fine’, ‘finer’, or ‘extra fine’, the exact and the finite-element solutions are extremely consistent, taking into account that the accuracy, depending on the nature of the equations, can be very sensitive to mesh resolution. This consistency confirms the correct finite-element implementation of the symmetric and simply supported boundary conditions and the adequacy of mesh resolution for the non-reinforced condition. Note that all present finite-element simulations are stationary and involve linear shape functions and tetrahedral elements. On a computing workstation with 28 computing 2 GHz cores and 64 GB of RAM, simulations in the present report can take between 15 minutes to a few hours to complete, depending on the specific simulation case.

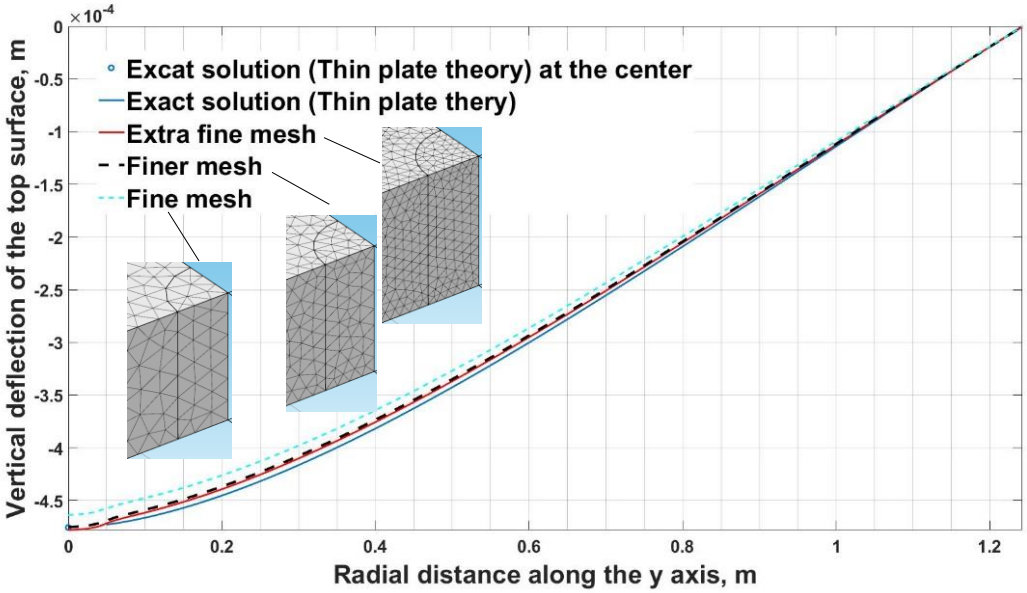

Figure 30. Exact and approximate (finite-element) solutions for deformation are consistent for all three mesh resolutions. This consistency confirms the implementation of the computational boundary and symmetry conditions and the adequacy of the mesh resolution for the non-reinforced case.

5.2. Estimation of the effective elastic modulus of ice

The most challenging part of the present study was the estimation of the effective elastic modulus (apparent Young’s modulus) for the tests described earlier in this report. This challenge is mainly due to the complex mechanics of ice and, thus, because of the inherent uncertainties associated with an idealized model. Moreover, in the testing, additional instrumentation would have helped in better documenting the ice response. The recoverable deformation of ice is due to two mechanisms: elasticity and delayed elasticity (Jellinek and Brill, 1956, Sinha, 1977). For the present computational numerical simulations, and since the ice is modeled as a linear elastic homogenous and isotropic material, a single modulus for ice is needed, which is strictly related to the pure elastic response of a material. For this reason, in the context of the recoverable response of ice, the term effective elastic modulus (or apparent Young’s modulus) is used. The effective elastic modulus of ice depends on many factors including crystal structure, temperature, and strain rate of ice. Note that the same consideration applies to the Poisson’s ratio of ice. However, because of the smaller sensitivity of the ice deflection to Poison’s ratio compared with the Young’s modulus, we simply take a nominal value of Poisson’s ratio for ice, which is 0.33.

Test E1 will be used as the first test case, to determine the effective elastic modulus. It was a non-reinforced ice plate approximately 0.11 m in thickness. The support frame was partially inside the ice by approximately 0.046 m, *i.e.* this was the value for ‘B’ in Figure 20. As mentioned earlier, the deflection of the top surface of the plate was measured at six locations along the radius of the plate. We calibrated the effective elastic

modulus of the ice in the simulations to reach an acceptable estimate of deflections consistent with the experimental measurements of the deflections. The boundary conditions for this test case was assumed to be fixed edges in contact with the frame ('N' in Table 1). Only half of the frame's thickness (*i.e.* 0.012 m) in the horizontal direction was considered in this simulation (Figure 32).

Figure 33 shows how the simulated vertical deflection of the ice for different effective elastic moduli compares with the measured deflections. None of the simulated cases generated deflections consistent with all deflection measurements. However, when the effective elastic modulus is 3 GPa, the simulated deflections for measurements that are closer to the center of the plate were more consistent with observations. The discrepancy between observed and modeled deflections could be due to measurement inaccuracies for the ice thickness and for the depth of the frame inside the ice. It could also be attributed to differences between the actual boundary conditions and those assumed in the simulation.

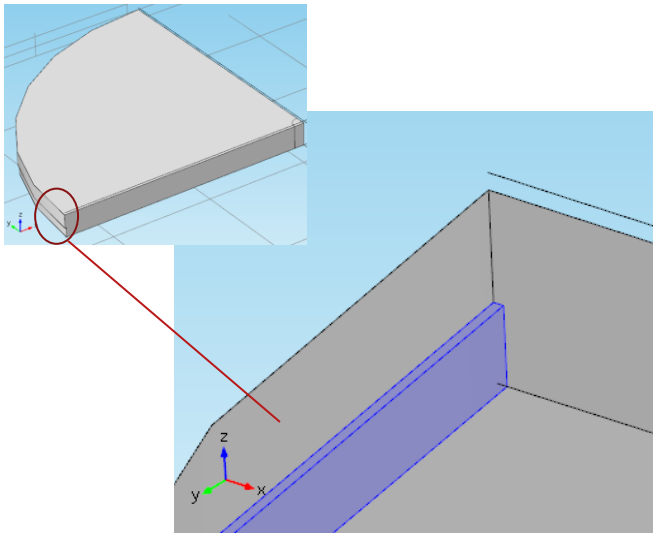

Figure 32. For calibrating the apparent Young's modulus of ice, the test E1 was used. The support frame was partially in ice and its contact with ice was simulated as fixed in all directions (highlighted in blue above). Note the xyz axes at the bottom left.

The first peak load for that test was approximately 9105N, recorded approximately after 2.2 seconds after the time of load application. That is the force that was used in this simulation. When the effective elastic modulus is taken to be 3 GPa (the red solid line in Figure 33), the extensional strain along the y axis at the bottom of the plate at the center was approximately 3.5×10^{-4}. The strain rate was then approximately 1.6E-4 s^{-1}. For columnar-grained ice (*i.e.* all the ice plates in the experiments) and at this strain rate, the effective elastic modulus is reported to be approximately 6 GPa at -20°C (Sinha, 1977). However, it is known that the effective modulus of ice is a strong function of the temperature and it generally decreases with increasing temperature (Sinha, 1989a).

For test E1, which was done with ice at approximately at -5°C, the 3 GPa estimate for the effective elastic modulus of ice is a reasonable starting point. Unless mentioned otherwise, for the rest of the present report, the effective elastic modulus of ice is tentatively taken to be 3 GPa.

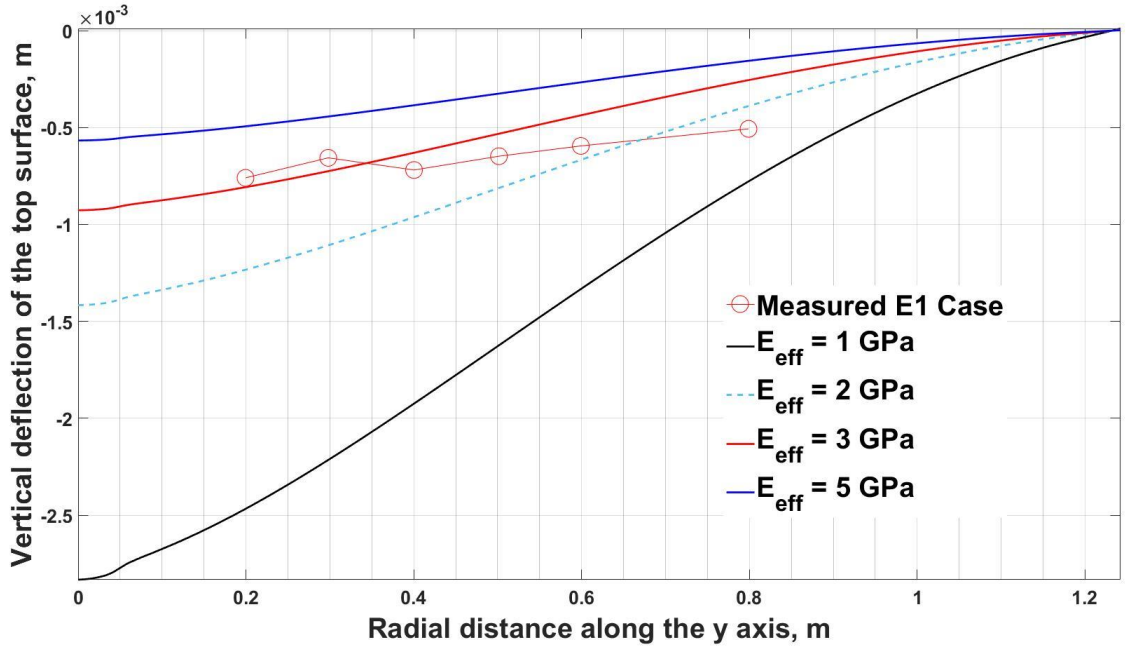

Figure 33. Measured versus simulated deflections for the E1 simulations, with different effective elastic moduli. The most consistent agreement with observations is the simulation with 3 GPa.

5.3. W3 – A test case for reinforced ice

For Test W3,, the seven 32-mm thick steel cables, in the experiments and in the simulation, were spaced symmetrically with respect to the ice plate center along the x axis. The distance between adjacent cables was 0.2 m and all cables were enclosed in the ice, 0.03 m above the bottom surface of the ice plate. The cables extended outside of the supporting frame and were not anchored. In the experiment, for that plate, the maximum force was approximately 2942 N. This is the input force for the present simulation.

Cables cannot bear any substantial bending moment, *i.e.* they will easily bend under their own weight. However, when they are enclosed within the ice plate, the confinement causes them to behave more like bars, which are stiff. Hence, for simplicity in the modeling exercise, the cables were modeled as bars. Also for the sake of simplicity, the cables were modeled as perfect circular cylinders in cross-section, although in reality, they are not. We do not expect these simplifications to cause a considerable deviation from reality. An effective elastic modulus of steel cables was assumed to be equal to the Young's modulus of steel (205 GPa). The reason why this is not the true modulus is that, according to Boroška et al. (2014), the Young's modulus of steel cables can be smaller than the Young's modulus of steel. Poisson's ratio of the cables was taken to be 0.28.

We conducted a brief mesh sensitivity study, so as to gain confidence in the mesh resolution required to adequately discretize the ice-cables system. The computational system forms a 'union' imposing a continuous deformation field and connectivity of finite-element nodes on the ice-cable interface. Three different meshes were tested: 'fine', 'finer', and 'extra fine' with a total number of elements being 4.6 M, 8.6 M, and 11.5 M, respectively. Figure 35 shows that even the 'fine' mesh discretizes the domain adequately (the deflection change when the mesh is finer is negligible). All three options can be used, depending on the desired output.

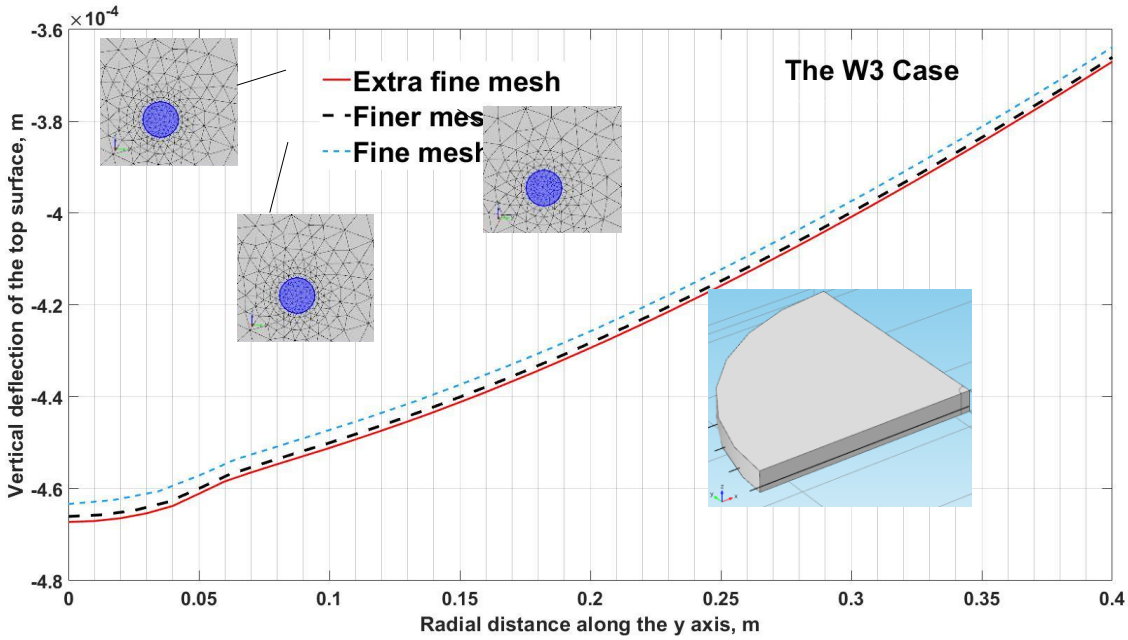

Figure 35. Cables and the ice have been discretized with enough elements so as not to have a strong mesh sensitivity between the three mesh resolutions given above. Note that the blue highlighted part of the mesh is the vertical cross section of a cable being 0.0032 m in diameter. The horizontal axis only shows part of a full ice plate radius. Note the xyz axes at the bottom left in the inset.

Figure 36 shows the outcome of this simulation and compares it with measured deflection for test W3. The measured deflection for test W3 is more consistent with the simulated case associated with an ice effective elastic modulus of 5 GPa compared to 3 GPa. This points to the possibility that the plate's effective modulus is somewhat higher than 3 GPa, or else that the model does not fully capture the reinforced ice response. Given that the input data from the laboratory tests was relatively crude, the former possibility is more likely. Based on the modeling, the reinforcement of the W3 case only negligibly reduces the initial elastic deflection of the ice sheet, regardless of whether the effective elastic modulus of ice is taken to be 3 GPa or 5 GPa.

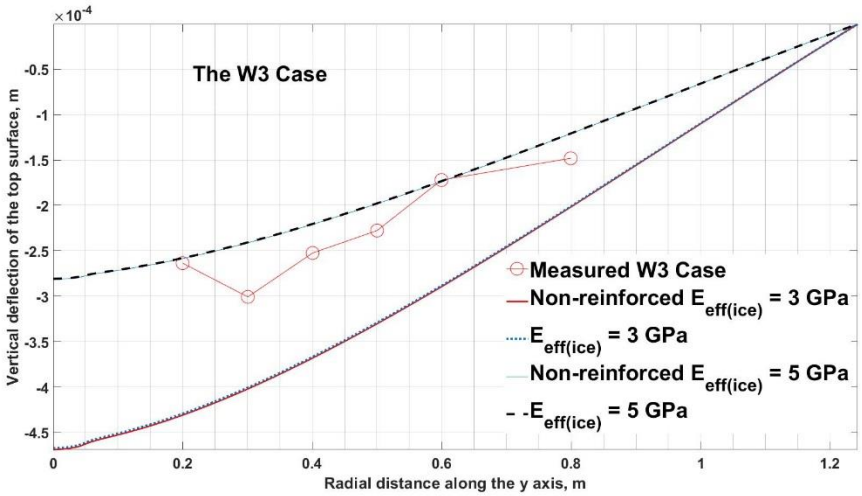

Figure 36. Vertical deflection with radial distance (see text for discussion. Note that both pairs of traces for the 3 GPa and 5 GPa are superimposed.

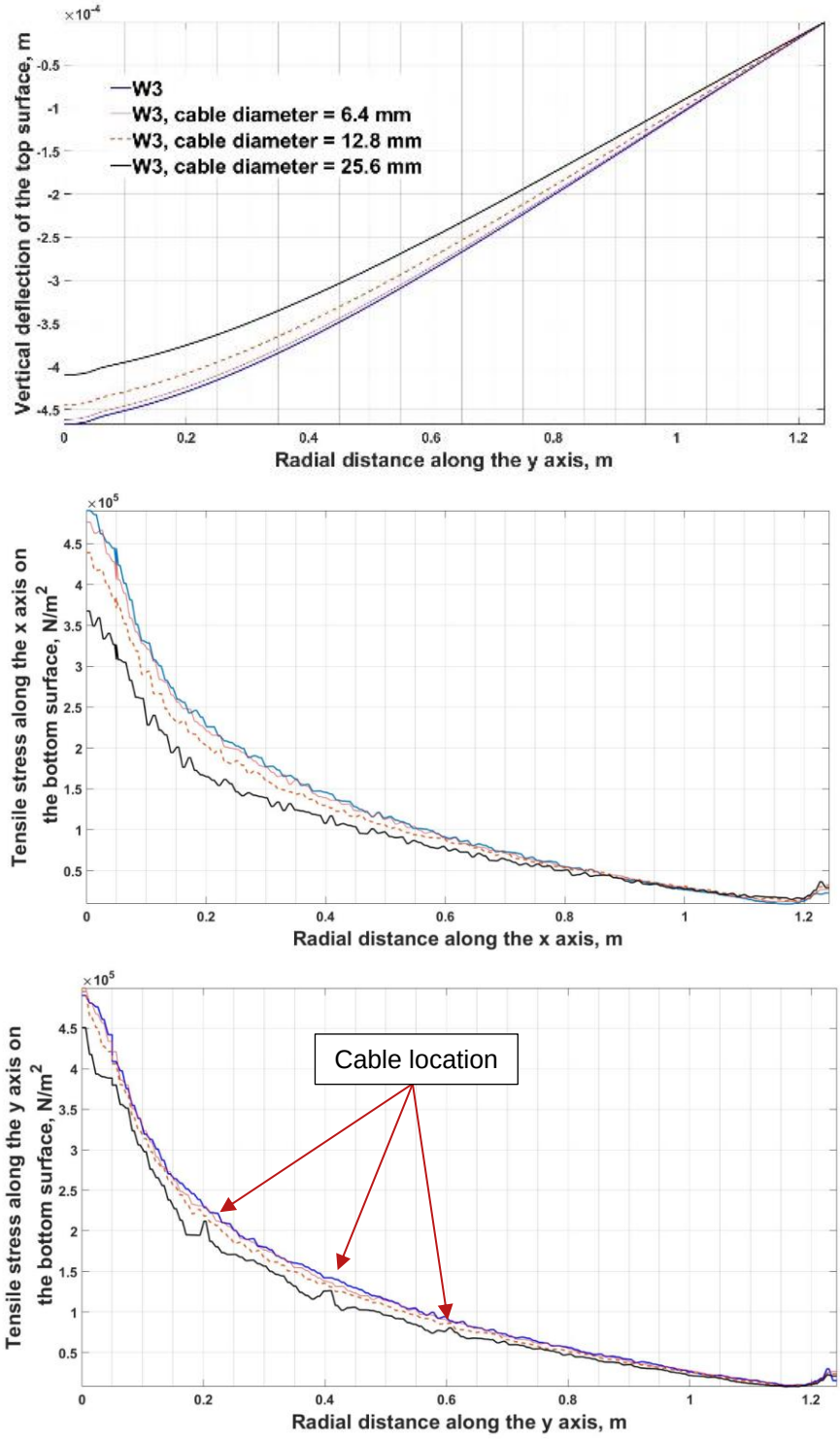

Figure 37. Top) An increase in the thickness of the cable improves the reinforcement effect for the W3 test. Middle) Tensile stress versus radial distance parallel to the cables. Bottom) Tensile stress versus radial distance perpendicular to the cables. Note in (c) the stress concentration in the ice along the lower surface of the ice plate for the case with the thickest cable.

We also briefly studied the impact of cable thickness on the reinforcement. As expected, the increase in the thickness leads to a higher stiffness of the system and hence reduction in the deflection and forces. Note that for the thickest cable simulated, the 0.0256 m, stress concentrations appear in the ice in the vicinity of the cables, as seen in Figure 37 (bottom).

5.4. W4 and E4

We also simulated tests W4 and E4. The W4 case consisted of reinforcement with ten 0.0064 m thick parallel cables distributed symmetrically with respect to the x axis and embedded in the ice 0.03 m above the bottom surface of the ice. The cables were spaced in a 0.15 m interval except the two cables at the center which were 0.3 m apart. The E4 case consisted of four cables of the same diameter and depth as the W4 case. The two central cables were apart 0.4 m and the spacing between each of the outer cables and the adjacent cable was 0.2 m. Simulation results of the E4 and W4 cases only show a minor difference in the vertical displacement of the ice plate (keeping in mind this is only for the initial elastic response, as mentioned before, not for the full loading history of the ice plate).

5.5. Other hypothetical scenarios for reinforcement

Three additional reinforcement scenarios were modeled (these were *not* tested in the laboratory). The purpose of this exercise was to explore other possibilities in terms of reinforcement options. Note that they do not factor in the important consideration of deployment and retrieval.

The first case is similar to test W3 with an additional seven cables perpendicular to the original cables located in a horizontal plane 0.04 m above the bottom surface of the ice. We refer to this scenario as the ‘cross-cable’ case. The second scenario is the reinforcement of the ice with a single 0.0032 m thick horizontal steel plate located 0.03 m above the bottom surface of the ice. We refer to this scenario as the ‘parallel-plate’ case. The third scenario consists of seven 0.0032 m thick vertical steel straps located at the same location as the original cables. We refer to this scenario as the ‘transverse-straps’ case (Figure 38).

Figure 39 compares how each of the hypothetical reinforcement cases impact the deflection and stresses. The cross-cable case is negligibly more desirable than the original W3 case, while the transverse-strap case shows substantial improvements. The parallel-plate case shows the strongest reinforcement where the maximum deflection and the maximum tensile stress on the bottom surface along the y axis are reduced by approximately 30% and 44%, respectively.

5.6. Summary of the computational modeling

A preliminary computational study was conducted to assess the performance of several different reinforcement scenarios for strengthening floating ice portions of winter roads. A few of these scenarios had been previously tested in NRC-Ottawa’s ice tank, and were used for validation and comparison purposes. Simulated scenarios included reinforcement with steel cables with different numbers strands and two thicknesses and two different distributions. Additional scenarios included reinforcement with a continuous solid steel plate embedded in ice parallel to its horizontal surfaces and another case with transverse steel straps.

Preliminary results associated with a 0.12 m thick ice plate with a diameter of approximately 2.5 m generally suggest that:

1. Steel cables do not reinforce ice unless their diameter is thick enough, say 0.0128 m and above. This was independent of the simulated number of reinforcing cables being 4, 7, and 10 cable strands. If the cables are very close to the ice bottom surface, the stress concentration in ice might be considerable.
2. Even a thin horizontal steel plate reinforces the ice in a substantial manner.
3. That is also the case for a system of multiple thin transverse steel straps.

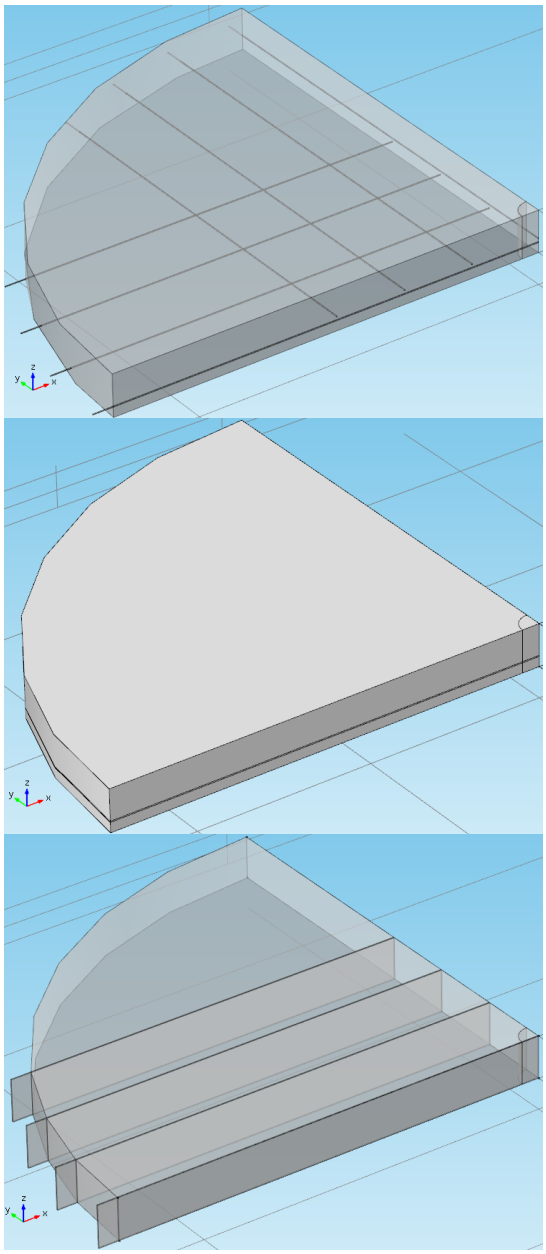

Figure 38: Three hypothetical scenarios: Top) The cross-cable case. Middle) The parallel-plate case. Bottom) The transverse-strap case.

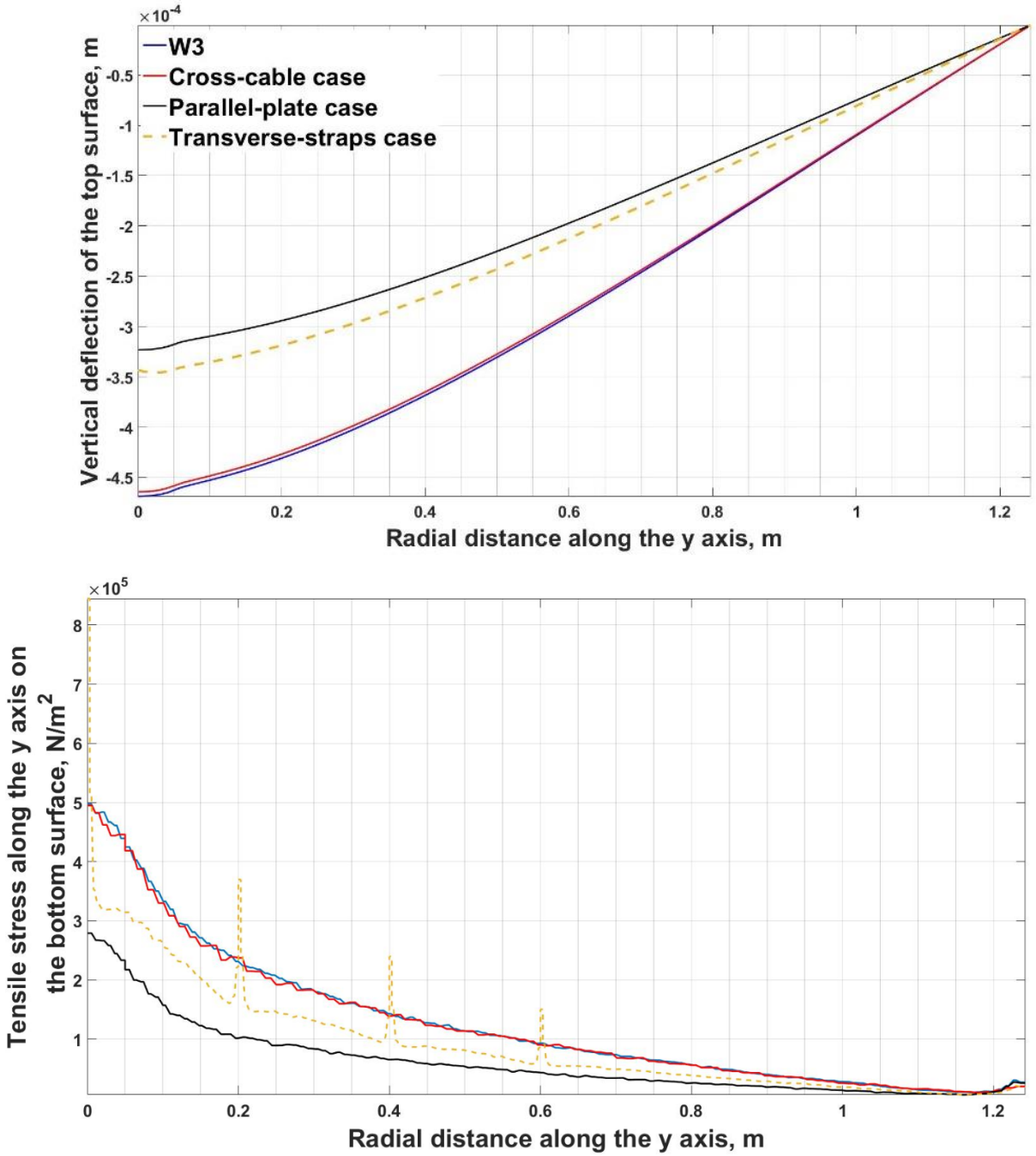

Figure 39: Top) Vertical deflection and tensile stress at the bottom of the plate for the three hypothetical scenarios. Bottom) Stresses in the steel reinforcement as the parallel-plate case is the most desirable of the three cases. Note the peaks in the stress for the transverse-straps case are stresses in the steel.

6. Conclusion

The ability for a floating ice cover to safely support the weight of vehicles under a wide variety of circumstances is a very important element in the design and operation of a winter road operation. In the 1950's and 1960's, Dr. Lorne Gold, a researcher at NRC, produced a study to guide design. His work is still being used today in most guidelines. Since then, there has been very little progress on that front. This report has provided introductory information on the considerations for determining ice thickness for safe ice road operations, and has introduced the concept of ice reinforcement to mitigate the effects of climate change that may lead to increased breakthroughs or decreased operability of ice roads. Finally, it has focused upon demonstrating the use of computational modelling to support the assessment of ice cover response to loading conditions.

Advances in computational modeling (Lau, 2017) opens the way to a new, relatively inexpensive research avenue. When fully validated against measurements, computational approaches such as the one described herein, are practical and inexpensive in assessing different hypothetical scenarios for ice cover reinforcement. With relative ease, they can be adopted to study reinforcement effectiveness of different materials, their distributions, and orientations. Examples could include studying the applicability of polymers or metal grids or naturally available material such as wood, including novel ones, such as carbon fiber reinforced polymer grids (e.g. Wu et al., 2019). Computational methods could also look at natural ice roads, their thickness variations, crack network distribution and density, etc. Software packages other than COMSOL capable of finite-element modeling, with applications in solid/structural mechanics, could be used for that purpose. These include:

- FreeFem++: freefem.org/ (open source)
- CalculiX: calculix.de/
- Code Aster: https://www.code-aster.org/spip.php?rubrique2

This report is also intended to inform researchers not yet familiar with these structures on the challenges at hand. They are encouraged to further explore the capability of this approach, and to experiment with various reinforcement scenarios and materials. This could provide a basis for determining what scenarios could be worthy of validation with real ice in a laboratory or another controlled environment.

7. Acknowledgements

The work reported herein is part of a project that was financed by Infrastructure Canada (INFC), Transport Canada's Northern Transportation Adaptation Initiative (NTAI) Program, Crown Indigenous Relations and Northern Affairs Canada (CIRNAC), and the Arctic Program of the National Research Council of Canada.

8. References

Aandahl, R.Z., Stadler, T., Sisson, S.A. and Tanaka, M.M., 2014. *Exact vs. approximate computation: Reconciling different estimates of Mycobacterium tuberculosis epidemiological parameters*. Genetics 196, p. 1227-1230.

Babaei, H., van der Sanden, J., Short, N. and Barrette, P., 2016. *Lake ice cover deflection induced by moving vehicles: Comparing theoretical results with satellite observations*, Transportation Association of Canada (TAC), Toronto.

Barrette, P., Charlebois, L. and Butt, B., 2019. *Reinforcement of ice covers for transportation: Material investigation and preliminary laboratory testing*. OCRE-TR-2018-031. National Research Council. Ottawa.

Barrette, P.D., 2015. *Overview of ice roads in Canada: Design, usage and climate change mitigation*. OCRE-TR-2015-011. National Research Council of Canada. Ottawa.

Bergan, P.G., Cammaert, G., Skeie, G. and Tharigopula, V., 2010. *On the potential of computational methods and numerical simulation in ice mechanics*. IOP Conference Series: Materials Science and Engineering, 10. IOP Publishing.

BMT Fleet Technology, 2011. *Ice bearing capacity manual*. Ottawa, Canada.

Boroška, J., Pauliková, A. and Ivančo, V., 2014. *Determination of elastic modulus of steel wire ropes for computer simulation*. Applied Mechanics and Materials, 683, p. 22-27.

Cederwall, K., 1981. *Behaviour of a reinforced ice-cover with regard to creep*, Proceedings of the 6th International Conference on Port and Ocean Engineering under Arctic Conditions (POAC), Quebec City, Canada, pp. 562-570.

Charlebois, L. and Barrette, P., 2019. *Ice reinforcement: Selection criteria for winter road applications and outcomes of preliminary testing*, Proceedings of the 18th International Conference on Cold Regions Engineering and of the 8th Canadian Permafrost Conference, Quebec City, pp. 119-127.

COMSOL AB, 2014. *COMSOL Multiphysics® v. 5.0 - Structural Mechanics Module User's Guide*, Stockholm, Sweden, p. 714-741.

CRREL, 2006. *Ice Engineering Manual*. EM 1110-2-1612. Department of the Army, U.S. Army Corps of Engineers. New Jersey.

CSAO, 2009. *Construction Health and Safety Manual*. Construction Safety Association of Ontario. Etobicoke, Canada.

CSST, 1996. *Travaux sur les champs de glace*. DC 200-640 (96-12). Gouvernement du Québec.

Dinvay, E., Kalisch, H. and Părău, E.I., 2019. *Fully dispersive models for moving loads on ice sheets*. Journal of Fluid Mechanics, 876, p. 122-149.

Frederking, R.M.W. and Gold, L.W., 1976. *The bearing capacity of ice covers under static loads*. Canadian Journal of Civil Engineering, 3, p. 288-293.

Gold, L.W., 1960. *Field study on the load bearing capacity of ice covers*, Woodlands Reviews. Canadian Pulp and Paper Association, Montreal, pp. 153-158.

Gold, L.W., 1971. *Use of ice covers for transportation*. Canadian Geotechnical Journal, 8, p. 170-181.

Gold, L.W., 1993. *The Canadian Habbakuk Project - A project of the National Research Council of Canada*. Lochem Prepress and Periodiekenservice, The Netherlands, 323 p.

Government of Manitoba, 2014. *Specifications for construction of a winter truck road*. Report no. 1250.

Government of the NWT, 2015. *Guidelines for safe ice construction*. Department of Transportation, Yellowknife, Canada, pp. 44.

Haynes, F.D., Collins, C.M. and Olson, W.W., 1992. *Bearing capacity tests on ice reinforced with geogrid*. Special Report 92-28.

Hori, Y. and Gough, W.A., 2018. *The state of Canadian winter roads south of the 60th parallel: historical climate analysis and projected future changes based on the climate model projections*. University of Toronto. Toronto.

Hori, Y., Gough, W.A., Butler, K. and Tsuji, L.J.S., 2017. *Trends in the seasonal length and opening dates of a winter road in the western James Bay region, Ontario, Canada*. Theoretical and Applied Climatology, 129, p. 1309-1320.

IHSA, 2014. *Best practices for building and working safely on ice covers in Ontario*. Mississauga, Ontario.

Jellinek, H.H.G. and Brill, R., 1956. *Viscoelastic properties of ice*. Journal of Applied Physics, 27(10), p. 1198-1209.

Kuehn, G.A. and Nixon, W.A., 1988. *Reinforced ice: Mechanical properties and cost analysis for its use in platforms and roads*, Proceedings of the 7th International Conference on Offshore Mechanics and Arctic Engineering (OMAE). The American Society of Mechanical Engineers (ASME), Houston, pp. 193-200.

Lau, M., 2017. *Numerical modeling of ice roads: an annotated bibliography*. OCRE-LM-2017-006. National Research Council. Ottawa.

Masterson, D.M., 2009. *State of the art of ice bearing capacity and ice construction*. Cold Regions Science and Technology, 58, p. 99-112.

Michel, B., Drouin, M., Lefebvre, L.M., Rosenberg, P. and Murray, R., 1974. *Ice bridges of the James Bay Project*. Canadian Geotechnical Journal, 11, p. 599-619.

Nixon, W.A. and Weber, L.J., 1991. *Flexural strength of sand-reinforced ice*. Journal of Cold Regions Engineering, 5(1), p. 14-27.

RSI, 2014. *Tibbitt to Contwoyto Mining Road - Historical climate analysis*. Ottawa.

Sinha, N.K., 1977. *Effective elasticity of ice*, Workshop on the Mechanical Properties of Ice. Technical Memorandum 121, Calgary, Canada, pp. 112-123.

Sinha, N.K., 1989a. *Elasticity of natural types of polycrystalline ice*. Cold Regions Science and Technology, 17, p. 127-135.

Sinha, N.K., 1989b. *Microcrack-enhanced creep in polycrystalline material at elevated temperature*. Acta Metallurgica, 37(11), p. 3107-3118.

Sinha, N.K. and Cai, B., 1996. *Elasto-delayed-elastic simulation of short-term deflection of fresh-water ice covers*. Cold Regions Science and Technology, 24, p. 221-235.

Squire, V.A., Hosking, R.J., Kerr, A.D. and Langhorne, P.J., 1996. *Moving loads on ice plates*. Kluwer Academic Publications.

Timoshenko, S. and Woinowsky-Krieger, S., 1959. *Theory of Plates and Shells*. McGraw-Hill Book Company, Toronto, 580 p.

van der Sanden, J.J. and Short, N.H., 2016. *Radar satellites measure ice cover displacements induced by moving vehicles*. Cold Regions Science and Technology, 133, p. 56-62.

Van Der Vinne, G., Lanteigne, M. and Snyder, J., 2017. *Measurement of ice covers under moving loads*, 19th Workshop on the Hydraulics of Ice Covered Rivers. CGU HS Committee on River Ice Processes and the Environment (CRIPE), Whitehorse, Canada.

Wu, Y., Liu, X., Chen, B., Li, Q., Luo, P. and Pronk, A., 2019. *Design, construction and monitoring of an ice composite shell structure*. Cold Regions Science and Technology, 106.

Young, W.C. and Budynas, R.G., 2002. *Roark's formulas for stress and strain*. McGraw-Hill, Toronto.